OPEN ACCESS

Orapuh Journal

ORIGINAL ARTICLE

Journal of Oral & Public Health

GIS-Based Aquifer Vulnerability Assessment Using DRASTIC and Susceptibility Index Models (SI): Funa Catchment, Kinshasa, Democratic Republic of the Congo

Iyeli, L. P.[1,2], Ndongela, M. J.[4], Mfumu, K. A.[3], Tangou, T. T.[1,2,3], Gizanga, V. R.[2], Makanzu, I. F.[4,5]

[1]*CBRN Centre of Excellence, Ministry of Higher Education, University, Scientific Research and Innovation, Democratic Republic of the Congo* [2]*Department of Environmental Sciences, Faculty of Sciences and Technologies, University of Kinshasa, Kinshasa XI, Democratic Republic of the Congo* [3]*Department of Soil Physics and Hydrology, Commissariat Général à l'Energie Atomique (CGEA), Democratic Republic of the Congo* [4]*Unit of Disaster Risk Management, Department of Geosciences, Faculty of Sciences and Technologies, University of Kinshasa, Kinshasa XI, Democratic Republic of the Congo* [5]*Unit of Geomorphology and Remote Sensing, Center for Research in Geological and Mining Research (CRGM), Kinshasa I, Democratic Republic of the Congo*

ARTICLE INFO

Received: *05 June 2026*
Accepted: *22 August 2026*
Published: *03 November 2026*

Keywords:
Aquifer vulnerability, DRASTIC, Susceptibility Index, groundwater governance, nitrates, Kinshasa

Peer-Review: *Externally peer-reviewed*

© 2026 The Authors.

Re-use permitted under CC BY-NC 4.0
No commercial re-use or duplication.

Correspondence to:
Plamedi IYELI LOBOTA
plamedi.iyeli@unikin.ac.cd

To cite:
Iyeli, L. P., Ndongela, M. J., Mfumu, K. A., Tangou, T. T., Gizanga, V. R., Makanzu, I. F. (2026). GIS-based aquifer vulnerability assessment using DRASTIC and Susceptibility Index Models (SI): Funa catchment, Kinshasa, Democratic Republic of the Congo. *Orapuh Journal, 7*(10), e1491. https://doi.org/10.4314/orapj.v7i10.91

ISSN: *2644-3740*

Published by ***Orapuh, Inc.***, F. Gaye Res., Sukuta-Jamisa, Greater Banjul, The Gambia.

Editor-in-Chief: *Prof. V. E. Adamu (editor@orapuh.org)*

ABSTRACT

Introduction
Water shortages and rapid population growth force residents in Kinshasa to rely heavily on groundwater. However, inadequate governance and management of this resource pose severe public health risks to consumers.

Purpose
This study mapped and evaluated the intrinsic and specific vulnerability of the aquifer system within the Funa catchment using Geographic Information System (GIS)-based DRASTIC and Susceptibility Index (SI) models to inform local and regional groundwater governance.

Methods
Physicochemical and parametric methods—including standard DRASTIC, land-use calibrated DRASTIC (DRASTICLU), and SI models—were implemented using ArcGIS 10.5. The input datasets comprised hydrogeological, climatic, topographic, and land-use parameters. In situ nitrate concentrations were sampled from 36 boreholes to validate specific vulnerability maps. Model validation and accuracy were further assessed using map removal sensitivity analysis, single-parameter sensitivity analysis, convergence analysis, and coincidence rates.

Results
The standard DRASTIC model classified the study area into three vulnerability zones: low (34.37%), moderate (54.56%), and high (11.07%). The SI model identified four vulnerability zones (low, moderate, high, and very high), with 83.46% of the area categorized as high. The DRASTICLU model also delineated four classes, identifying 8.40% of the catchment as very high vulnerability. The coincidence rate between observed borehole nitrate concentrations and vulnerability classes was 41.70% for the DRASTICLU model and 33.30% for the SI model.

Conclusion
The low-lying plain areas exhibit the highest aquifer vulnerability due to shallow water tables, gentle topographic slopes, and intense anthropogenic pressure. The relatively low coincidence rates reflect uneven spatial distribution of monitoring wells and localized differences in well construction and management. Establishing structured groundwater governance and management frameworks at local, regional, and national levels is strongly recommended.

INTRODUCTION

In recent decades, global water quality degradation has emerged as a critical environmental concern, exacerbated by limited freshwater availability and rapid population growth (UNESCO World Water Assessment Programme, 2016). Because surface water bodies interact directly with anthropogenic activities, they are significantly more vulnerable to pollution than subsurface aquifers. Consequently, groundwater serves as the primary water source for drinking, commercial, and agricultural uses globally (Ifediegwu & Chibuike, 2021; Rahman, 2008). Historically, groundwater quality was assumed to be naturally protected by overlying soil profiles and unsaturated vadose zones, which act as physical and chemical filters against surface-derived contaminants (Matungila et al., 2025). However, recognition of progressive groundwater degradation was long delayed (Meyzonnat, 2012).

Aquifer vulnerability refers to the likelihood that a contaminant or group of contaminants will migrate from the surface and reach the water table. It quantifies the intrinsic lack of natural protection based on local hydrogeological characteristics (Simboro, 2016) or the chemical dynamics of specific pollutants (Amharref et al., 2007). Groundwater protection studies distinguish between *intrinsic* and *specific* vulnerability. Intrinsic vulnerability is determined solely by physical, geological, hydrogeological, and climatic parameters governing fluid infiltration and solute transport through the unsaturated zone, such as soil texture, vadose zone lithology, topographic slope, and effective precipitation (Seguin et al., 2002). These intrinsic factors govern three primary subsurface dynamics: contaminant attenuation and travel time, flow dynamics within the vadose zone, and residual pollutant concentration upon entering the saturated zone (Rizka, 2018). Conversely, specific vulnerability accounts for the chemical properties of specific pollutants, their interactions with the subsurface media, and spatial land-use patterns resulting from human activities (Ewodo et al., 2016). Specific vulnerability is typically mapped in two-dimensional formats to guide land-use planning and prevent groundwater contamination (Meyzonnat, 2012).

Methodologies for assessing hydrogeological vulnerability are broadly grouped into three categories: overlay/index methods (parametric models), statistical models, and process-based mathematical models (Chenini et al., 2015; Liggett & Talwar, 2009). Process-based models simulate physical and chemical attenuation mechanisms (Falasi, 2018; Frind et al., 2006; Neukum & Azzam, 2009), whereas statistical approaches evaluate empirical relationships. Despite inherent subjectivity in weight assignment (Hamza et al., 2015; Mfumu et al., 2016), index-overlay parametric methods remain the most widely applied due to their computational efficiency and adaptability to regional datasets (Ifediegwu & Chibuike, 2021; Ojeda-Olivares et al., 2020). Subjectivity in these models is increasingly minimized through sensitivity analyses, multi-model integration, and field validation using physicochemical or bacteriological indicators.

In the Democratic Republic of the Congo (DRC), despite possessing over 86,080 km² of internal surface water resources—representing 3.5% of the national territory (Ndembo, 2009)—inadequate infrastructure creates severe drinking water insecurity (Falasi, 2018; Ilunga et al., 2013; Kasuku et al., 2016; Matungila, 2023; Ndolo, 2015). In the city-province of Kinshasa, particularly across the southwestern hills and central plains, urban water distribution by the national utility (REGIDESO) is severely limited or non-existent due to network degradation and gully erosion sedimentation (Makanzu Imwangana et al., 2015). Consequently, residents rely on unmonitored private boreholes, artificial wells, and natural springs. Most private wells lack standard sanitary protection zones, exposing them to direct pollution.

The Funa River catchment encompasses a major urbanized drainage basin in Kinshasa. Rivers originating in the southern high-altitude areas are impacted by agricultural practices and severe gully erosion (Matumona Seya et al., 2025). As these streams cross the densely populated plain, water quality declines significantly due to untreated domestic sewage, solid waste accumulation, industrial effluents, and healthcare wastes (Gizanga et al., 2016; Lemba, 2013; Mindele, 2016). The underlying hydrogeological structure consists of an unconfined alluvial aquifer in direct hydraulic connection with surface streams and a deeper semi-confined aquifer supplying local wells. Pervasive surface contamination, combined with permeable sandy formations, unsealed pit latrines

(Massawe et al., 2017), open refuse dumps, and uncontrolled erosion-control waste infills (Makanzu Imwangana et al., 2022, 2025), presents a severe contamination risk to these aquifers.

To address these challenges, this study addresses the following central question: How can combining GIS techniques, parametric models (DRASTIC and SI), and physicochemical field sampling evaluate aquifer vulnerability in the Funa catchment to support sustainable groundwater protection?

The overarching objective of this study is to map and evaluate the intrinsic and specific vulnerability of the Funa catchment aquifer system using integrated standard DRASTIC, DRASTICLU, and Susceptibility Index (SI) models. The specific objectives are to:

1. Identify, parameterize, and map key environmental and hydrogeological factors governing groundwater vulnerability across the catchment.
2. Delineate intrinsic and specific vulnerability zones using DRASTIC, DRASTICLU, and SI parametric models.
3. Validate and calibrate spatial vulnerability maps using in situ nitrate (NO_3^-) field measurements from local boreholes.
4. Propose strategies for the management and protection of groundwater resources..

METHODS

Study Area

The Funa catchment is located east of central Kinshasa, between longitudes 15°15'14.5" E and 15°20'59.5" E and latitudes 4°19'14.5" S and 4°26'51.5" S **(Figure 1)**. The basin covers 70.5 km² with a perimeter of 45 km. Five primary tributaries—Bumbu, Kemi, Yolo, Nsadi, and Funa—drain the catchment across 14 administrative townships: Mont-Ngafula, Selembao, Makala, Bumbu, Ngiri-Ngiri, Kasa-Vubu, Kinshasa, Barumbu, Gombe, Ngaliema, Limete, Kalamu, Ngaba, and Lemba (Miti & Mukanu, 2021). Topographically, the southern section features steep hills reaching elevations up to 546 m above sea level, transitioning northward into low-lying floodplains with gentle slopes and elevations ranging between 269 m and 330 m **(Figure 2)**.

Figure 1:
Study area (a. Funa catchment area; b. Kinshasa City-Province; c. Democratic Republic of the Congo)

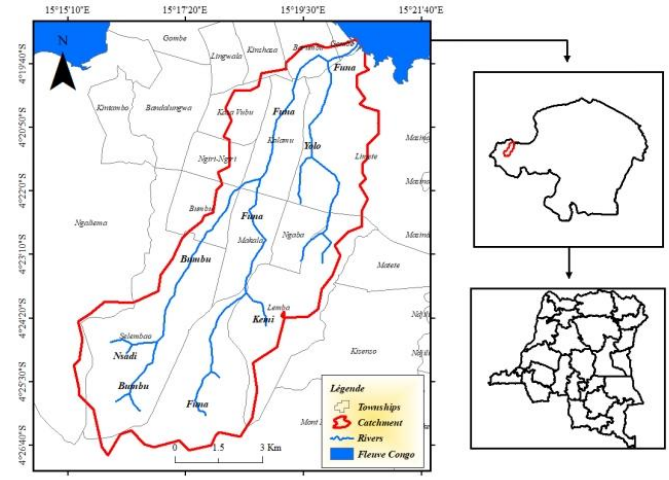
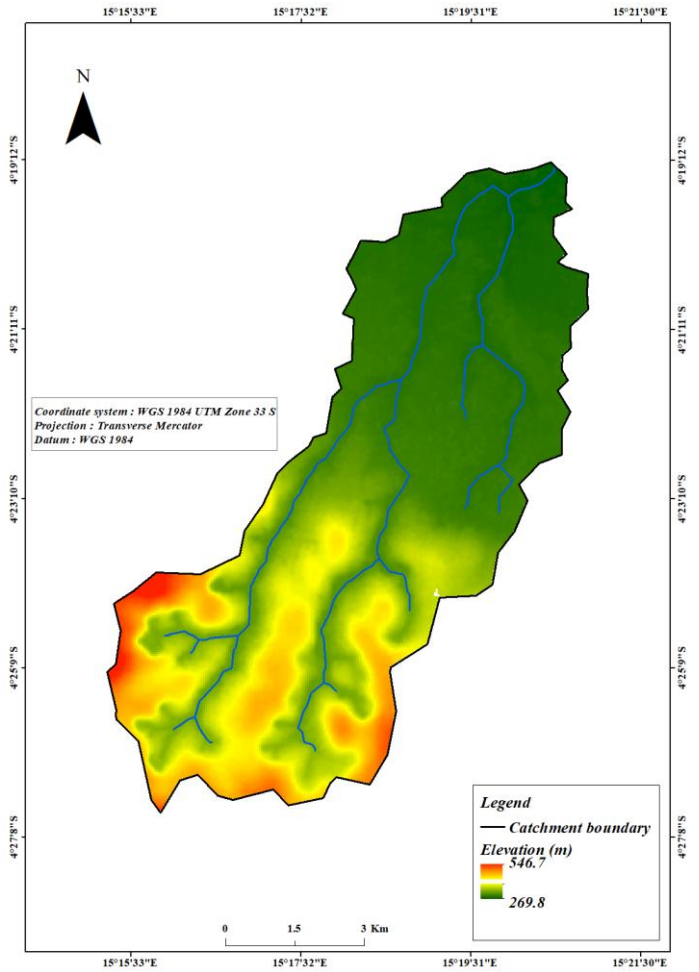


Figure 2:
Elevation Map



According to the Köppen-Geiger climate classification updated by Peel et al. (2007), Kinshasa experiences a tropical wet and dry climate (AW4). Mean annual precipitation exceeds 1,500 mm. Geologically, the area is dominated by Neogene ochre sands (Egoroff, 1974). Soils are predominantly categorized as Arenosols under the World Reference Base system (Courbe, 2023; Davies, 2015), comprising medium-terrace alluvium across the plains and poorly consolidated, highly erodible fine sands along hillslopes. Hydrogeologically, the region forms part of Kinshasa's central and eastern hydrogeological units (Aquater, 1987).

Urban land use varies from planned residential zones in the lowlands to highly dense, informal settlements along southern slopes. The catchment population was estimated at 3,764,066 in 2004 (Institut National de la Statistique, 2004) and is projected to reach approximately 20 million by 2026 based on an annual growth rate of 5.13%. High population density, insufficient sanitation infrastructure, market gardening along river valleys, and frequent rainfall-induced flooding contribute to heavy organic, nitrate, and chemical loadings.

DRASTIC and DRASTICLU Vulnerability Models

The DRASTIC model (Aller et al., 1987) evaluates intrinsic vertical aquifer vulnerability using seven weighted hydrogeological parameters: Depth to water table (**D**), Net recharge (**R**), Aquifer media (**A**), Soil media (**S**), Topography/Slope (**T**), Impact of the vadose zone (**I**), and Hydraulic Conductivity (**C**). Each parameter is assigned a rating (r) from 1 (least vulnerable) to 10 (most vulnerable) and a fixed weight (w) from 1 to 5 based on its relative importance in contaminant transport **(Table 1)**.

Table 1
Weights and Ratings for the Parameters of the Standard DRASTIC and SI Models in the Funa Catchment

Parameter	DRASTIC Weight	SI Weight	Class / Range	DRASTIC Rating	SI Rating
Depth to water table (m)	5	0.186	0–5	10	100
			5–15	9	90
			15–30	7	70
			30–50	5	50
			50–75	3	30
			75–100	2	20
			> 100	1	10
Net recharge (mm/year)	4	0.212	> 225	9	90
Aquifer media	3	0.259	Alluvial	8	80
			Sandstones	6	60
Soil media	2	–	Alluvial (sandy)	6	–
			Sandy	9	–
Topography (%)	1	0.121	0–2	10	10
			2–6	9	90
			6–12	5	50
			12–18	3	30
			> 18	1	10
Impact of the vadose zone	5	–	Alluvial	6	–
			Sandy + clay	3	–
Hydraulic conductivity (m/s)	3	–	1.5×10−7–5×10−5	1	–
			>5×10−5	2	–
Land use / Cover	5	0.222	Mixed forest	1	0
			Marshland	2	50
			Agriculture	4	70
			Peri-urban and rural	5	70
			Urban	8	75
			Wild dump	–	100

https://doi.org/10.4314/orapj.v7i10.91

The Standard DRASTIC Index (ID) is calculated as follows:

$$ID = (Dr \times Dw) + (Rr \times Rw) + (Ar \times Aw) + (Sr \times Sw) + (Tr \times Tw) + (Ir \times Iw) + (Cr \times Cw) \quad (1)$$

Where r represents the associated rating and w is the weight of each parameter. The vulnerability index values range from 23 to 226 in the standard version **(Table 2)**.

Table 2:
Vulnerability Index Classifications for the Standard DRASTIC Method According to Aller et al. (1987) and Engel et al. (1996)

Model	Vulnerability Index Range	Vulnerability Degree
DRASTIC (Aller et al., 1987)	<80	Very low
	80–120	Low
	121–160	Moderate
	161–200	High
	>200	Very high
DRASTIC (Engel et al., 1996)	<101	Low
	101–140	Moderate
	141–200	High
	>200	Very high

All parameters were processed in ArcGIS 10.5. Depth-to-water data were interpolated from borehole measurements. Net recharge (R) was estimated via

Thornthwaite water balance equations using precipitation (P), temperature (T), annual heat index (I), and monthly daylight correction factors (k):

$$ETP_{raw} = 16 \times \left(\frac{10T}{I}\right)^{a} \quad (2)$$

$$a = (6.75 \times 10^{-7} \times I^3) - (7.71 \times 10^{-5} \times I^2) + (1.792 \times 10^{-2} \times I) + 0.49239 \quad (3)$$

$$k = \frac{N}{30} \times \frac{d}{12} \quad (4)$$

$$ETP = k \times ETP_{raw} \quad (5)$$

$$R_{net} = P - ETP \quad (6)$$

Soil data were derived from the Central Africa Soil and Terrain Database (SOTERCAF v1.0). Lithological and vadose zone properties were obtained from the British Geological Survey Africa Groundwater Atlas. Topographic slopes were computed from 30 m SRTM digital elevation models (DEM). Hydraulic conductivity values were assigned based on hydrogeological literature for Kinshasa (Mfumu, 2016).

To account for anthropogenic impacts, the calibrated **DRASTICLU** model was developed by integrating a Land Use/Land Cover (**LU**) layer assigned a relative weight of w = 5 **(Table 1)**.

Susceptibility Index (SI) Model

The Susceptibility Index (SI) model (Ribeiro, 2000) evaluates specific aquifer vulnerability to agricultural and land-based contaminants (e.g., nitrates) across local and regional scales. It integrates five parameters: Depth to water table (**D**), Net recharge (**R**), Aquifer media (**A**), Topography (**T**), and Land Use (**OS**).

The SI score is computed as follows:

$$SI = (Dr \times Dw) + (Rr \times Rw) + (Ar \times Aw) + (Tr \times Tw) + (OSr \times OSw) \quad (7)$$

Land use was classified using the CORINE Land Cover framework (European Community, 1993). Parameter ratings and weights are detailed in **Table 1**, and SI vulnerability classes are defined in **Table 3**.

Table 3
Vulnerability Index Classifications for the Susceptibility Index (SI) Model

Vulnerability Degree	Vulnerability Index Range (SI)
Low	<45
Moderate	45–64
High	65–84
Very high	85–100

Physicochemical Analysis

To validate specific vulnerability maps, groundwater nitrate (NO_3^-) concentrations were measured in situ across 36 boreholes using Quantofix Nitrate colorimetric test strips (ranges: 0–10, 10–25, 25–50, 50–100, 100–250, and 250–500 mg/L). All field measurements were performed in triplicate to ensure analytical reliability.

Map Overlap, Convergence, and Coincidence Rate Analysis

Model convergence was evaluated in ArcGIS 10.5 using the *Tabulate Intersection* geoprocessing tool. To quantify agreement between spatial vulnerability models and empirical field data, the Coincidence Rate (T_c) was calculated by matching observed nitrate concentration classes (Low: 0-25 mg/L, Moderate:

25-50 mg/L, High: 50-500 mg/L) against mapped vulnerability classes **(Table 4)**:

$$Tc = \frac{(X1, Y1) + (X2, Y2) + (X3, Y3)}{\sum_{i=1}^{36} (Yi)} \times 100 \quad (8)$$

https://doi.org/10.4314/orapj.v7i10.91

Where X_i represents the model vulnerability class, Y_i represents the corresponding nitrate concentration class, n is the number of classes, and N is the total number of sampled boreholes (N = 36).

Table 4:
Coincidence Matrix for Model and Field Comparison

XY	Y1 (Low)	Y2 (Moderate)	Y3 (High)
X1 (Low)	X1,Y1	X1,Y2	X1,Y3
X2 (Moderate)	X2,Y1	X2,Y2	X2,Y3
X3 (High)	X3,Y1	X3,Y2	X3,Y3

Sensitivity Analysis

Sensitivity analyses were conducted to evaluate the influence of individual parameters on the calculated vulnerability indices (Lodwick et al., 1990; Napolitano & Fabbri, 1996).

1. **Map Removal Sensitivity Analysis (MRSA):** Measures the sensitivity (S) of the final vulnerability index upon removing one parameter layer at a time:

   $$S = (|V / N - V' / n| / V) \times 100 \quad (9)$$

   Where V is the unadjusted vulnerability index (all layers), V' is the index computed after removing one parameter layer, N is the total number of original layers, and n is the remaining number of layers (n = N - 1).

2. **Single-Parameter Sensitivity Analysis (SPSA):** Evaluates the effective (realized) weight (W_e) of each parameter relative to its theoretical weight:

   $$W = [(P_r \times P_w) / V] \times 100 \quad (10)$$

   Where P_r and P_w are the rating and theoretical weight assigned to parameter P, and V is the overall vulnerability index.

RESULTS

Application of the Standard DRASTIC Vulnerability Model

The calculated standard DRASTIC vulnerability indices range from 96 to 173 across the catchment. Applying standard classification thresholds yields three distinct vulnerability levels: low, moderate, and high **(Figure 3)**. The moderate vulnerability class is dominant, covering approximately 54.60% of the study area, and is primarily distributed across lowland alluvial plains and steep valley bottoms. Low vulnerability zones are largely restricted to the southern hilly uplands, whereas high vulnerability zones concentrate predominantly in the eastern sector of the alluvial plain.

When evaluated using the modified classification thresholds proposed by Engel et al. (1996), the spatial distribution shifts significantly: high vulnerability zones expand to encompass approximately 45.80% of the plain's aquifer system (**Figure 4**), while moderate vulnerability remains dominant across the southern hills (approximately 48.90%). The proportional area coverage for each vulnerability level under both classification schemes is summarized in **Table 5**.

Figure 3:
DRASTIC Index – Classified according to Aller et al. (1987)

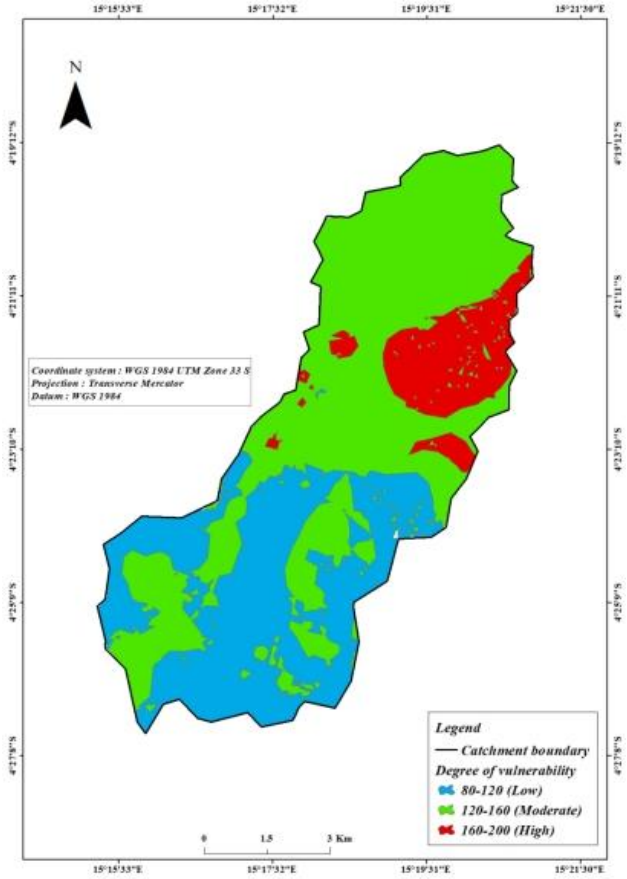
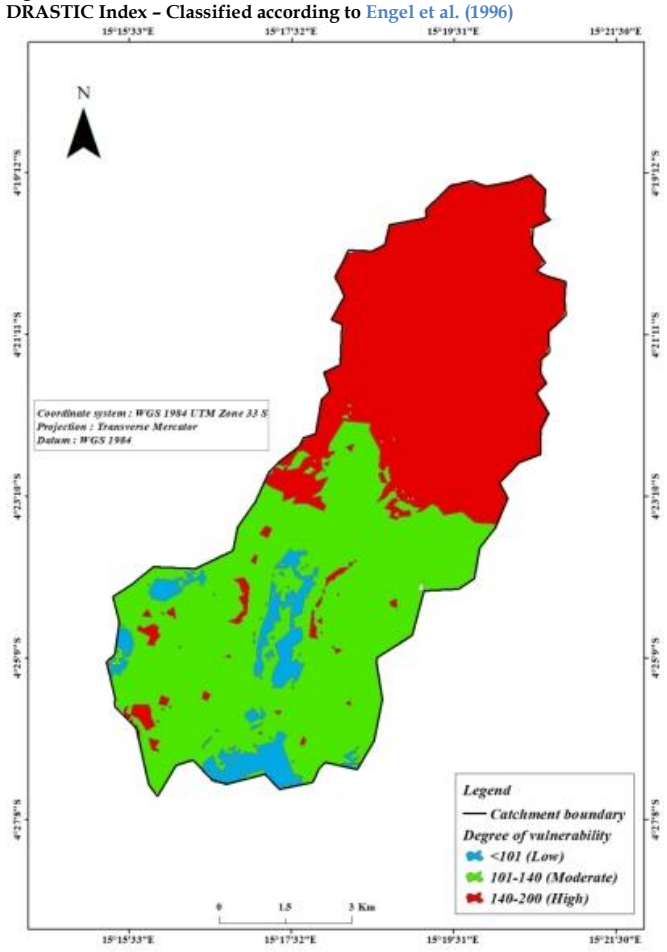


Table 5:
Spatial Extent of Vulnerability Degrees According to the Standard DRASTIC Model

Model	Vulnerability Index Range	Vulnerabilty Degree	Area (km²)	Area (%)
DRASTIC	96–120	Low	24.22	34.37
(Aller et al.,1987)	121–160	Moderate	38.44	54.56
	161–173	High	7.80	11.07
DRASTIC	96–100	Low	3.76	5.33
(Engel et al., 1996)	101–140	Moderate	34.45	48.89
	141–173	High	32.25	45.77

Figure 4:
DRASTIC Index – Classified according to Engel et al. (1996)



Application of the Susceptibility Index (SI) and Calibrated DRASTIC (DRASTICLU) Models

The Susceptibility Index (SI) model yielded vulnerability scores ranging from 39.50 to 87.50, delineating four vulnerability categories **(Figure 5, Table 6)**. High vulnerability dominates the SI outputs, covering 83.46% of the catchment.

Table 6:
Spatial Extent of Vulnerability Degrees According to the Susceptibility Index (SI) Model

Model	Vulnerability Index Range	Vulnerability Degree	Area (km²)	Area (%)
SI	38.5–44	Low	0.07	0.10
	45–64	Moderate	11.47	16.36
	65–84	High	58.48	83.46
	85–89.5	Very high	0.05	0.08

Figure 5:
SI Index – Classified

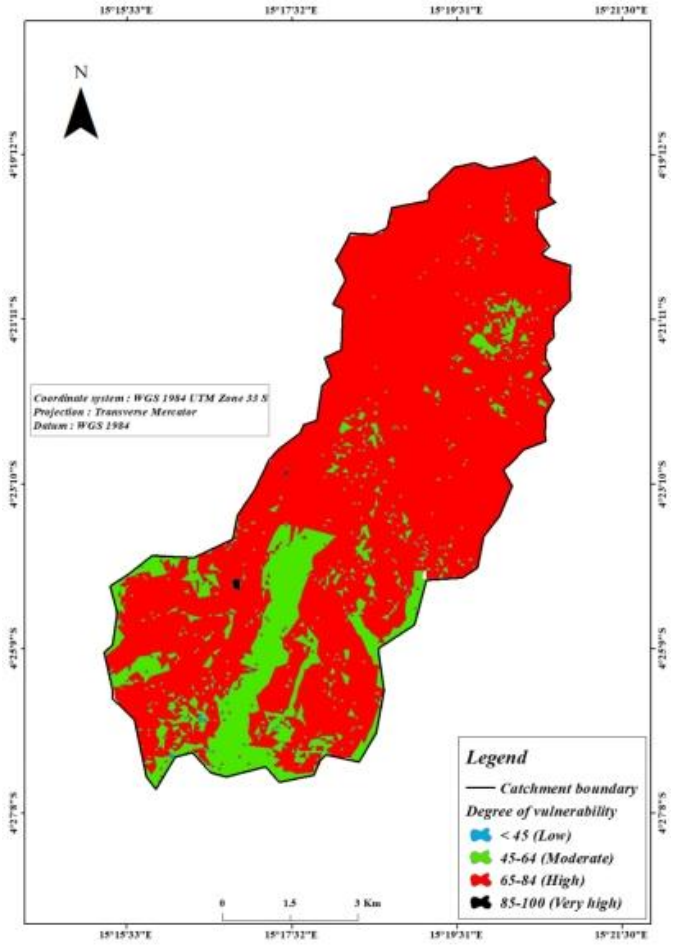
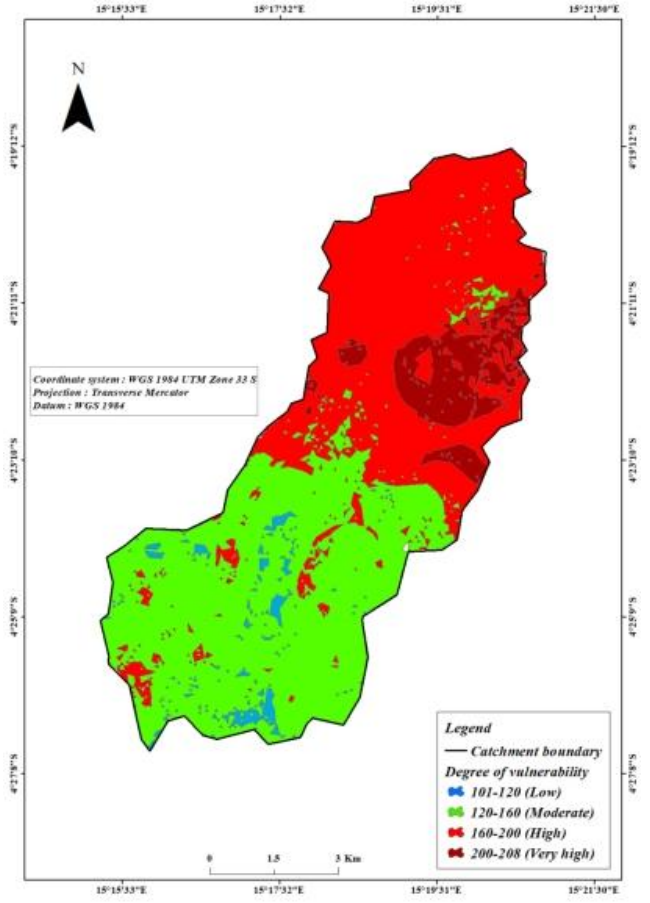


Table 7:
Spatial Extent of Vulnerability Degrees According to the Calibrated DRASTICModel (DRASTICLU)

Model	Vulnerability Index Range	Vulnerability Degree	Area (km²)	Area (%)
DRASTICLU	101–120	Low	1.37	1.90
	121–160	Moderate	33.60	48.10
	161–200	High	29.00	41.60
	200–208	Very high	5.90	8.40

Similarly, the land-use calibrated DRASTIC model (**DRASTICLU**) generated index values ranging from 101 to 208, grouped into four vulnerability classes **(Figure 6, Table 7)**. The very high vulnerability class accounts for 8.40% of the total area and is heavily concentrated within the low-lying plain.

Figure 6:
DRASTICLU index



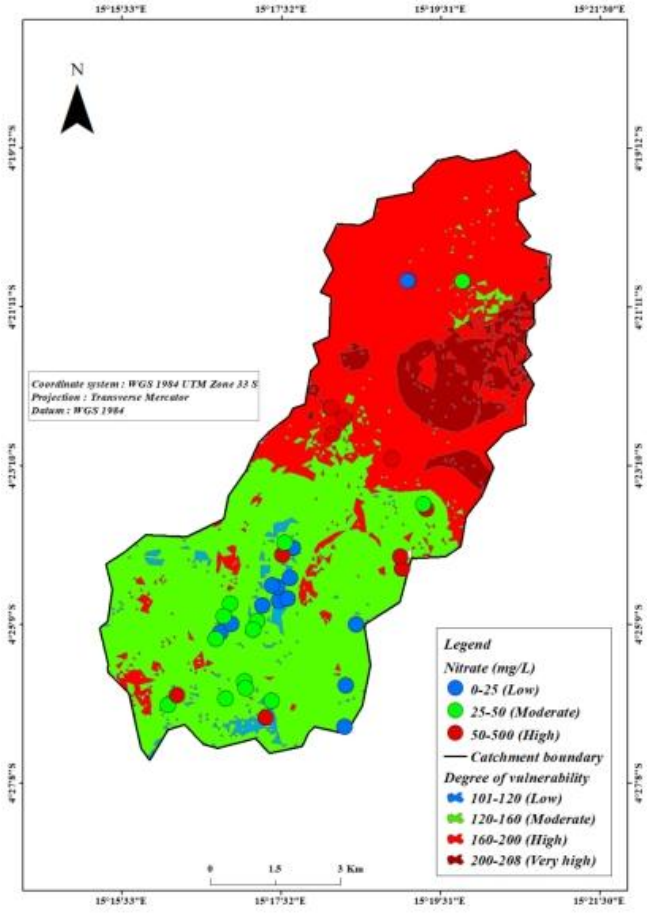
Groundwater Nitrate Concentration Mapping

In situ nitrate (NO_3^-) concentrations sampled across the 36 monitoring boreholes ranged from 0 to 500 mg/L. Among the sampled wells, 13 exhibited concentrations between 0 and 25 mg/L, 13 fell within the 26–50 mg/L range, and 10 exceeded 50 mg/L. Groundwater nitrate data were spatially overlaid onto the DRASTICLU and SI model maps **(Figures 7 and 8)** to evaluate empirical model accuracy. The observed nitrate concentration intervals across the 36 monitoring boreholes are detailed in **Table 8**.

Table 8
Spatial Coordinates of Monitoring Wells and Measured Nitrate Concentrations

Borehole ID	Latitude (S)	Longitude (E)	Water Table Depth (m)	Nitrates (NO_3^-, mg/L)
F1	-4.431082	15.284616	123	25–50
F2	-4.432535	15.284873	100	25–50
F3	-4.434608	15.280621	100	25–50
F4	-4.438589	15.288956	150	50–100
F5	-4.435138	15.290240	120	25–50
F6	-4.418480	15.287149	150	25–50
F7	-4.420236	15.286346	180	25–50
F8	-4.414324	15.291682	114	0–10
F9	-4.411400	15.291401	131	0–10
F10	-4.411048	15.290246	130	10–25
F11	-4.413819	15.293508	120	0–10
F12	-4.409528	15.294014	120	10–25
F13	-4.415247	15.288226	125	0–10
F14	-4.446848	15.281068	106	10–25
F15	-4.440556	15.305355	120	0–10
F16	-4.403227	15.294603	180	10–25
F17	-4.404693	15.292454	150	50–100
F18	-4.402237	15.292922	33	25–50
F19	-4.420944	15.279511	50	0–10
F20	-4.419133	15.281786	40	0–10
F21	-4.414872	15.281642	30	25–50
F22	-4.417553	15.280267	50	25–50
F23	-4.422183	15.278619	90	25–50
F24	-4.407634	15.317293	90	100–250
F25	-4.405068	15.316903	62	100–250
F26	-4.395126	15.322234	68	100–250
F27	-4.394119	15.321666	20	25–50
F28	-4.347677	15.329778	25	25–50
F29	-4.384740	15.315130	32	250–500
F30	-4.379540	15.302760	70	100–250
F31	-4.376240	15.305250	56	100–250
F32	-4.374060	15.302400	150	100–250
F33	-4.435970	15.268750	70	25–50
F34	-4.433910	15.270570	75	50–100
F35	-4.431920	15.305620	120	10–25
F36	-4.419150	15.307720	90	0–10

Figure 7:
Risk map DRASTICLU



https://doi.org/10.4314/orapj.v7i10.91

Figure 8:
Risk map SI index

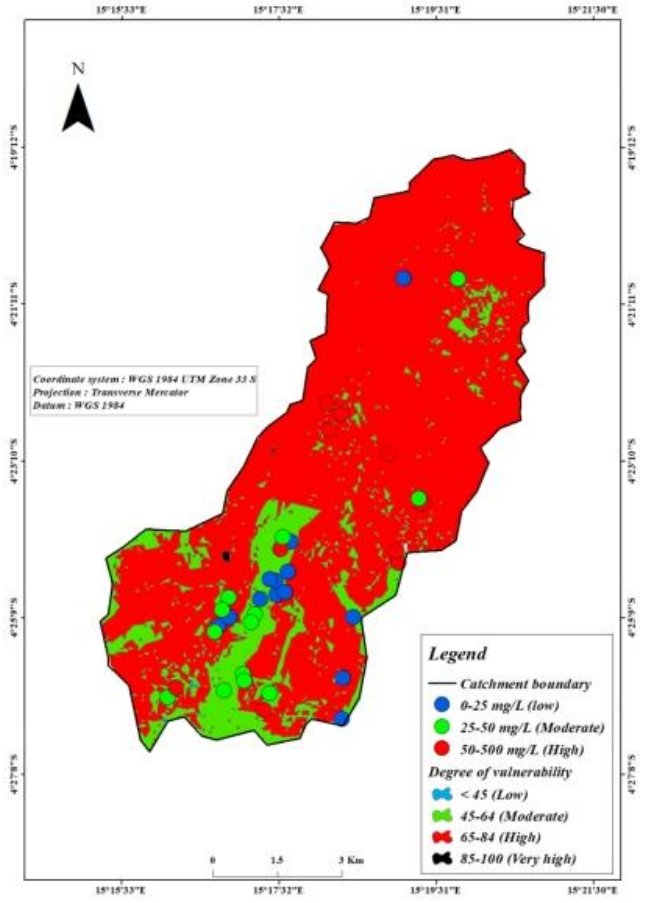
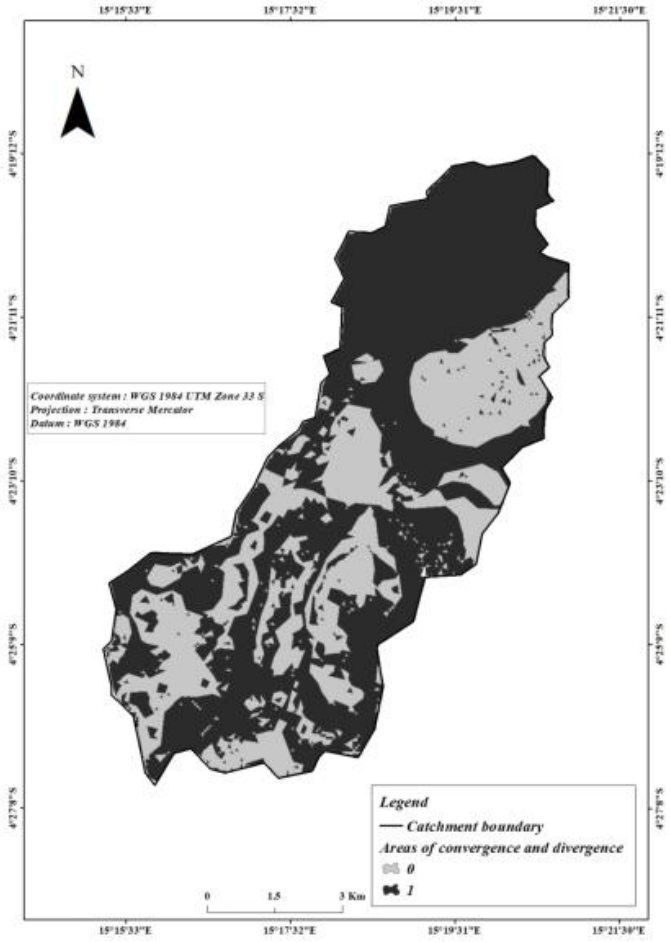


Figure 9:
Areas of agreement and disagreement between Aller's and Engel's classifications



Statistical and Sensitivity Analyses

Convergence, Divergence, and Coincidence Rate (T_c) Analysis

Cross-tabulation of the standard DRASTIC model against Engel et al.'s (1996) modified classification revealed notable discrepancies. Within the 24.20 km² classified as low vulnerability under the standard scheme, only 3.80 km².maintained low vulnerability under Engel's classification, with the remaining 20.40 km² reclassified as moderate vulnerability **(Table 9)**. Overall spatial agreement between the two classification methods covers approximately 25.60 km² (36.30%), whereas disagreement spans 45.00 km² (63.70%). **Figure 9** illustrates spatial convergence (0) and divergence (1) zones.

Table 9:
Convergence and Divergence Between Standard DRASTIC (Aller et al., 1987) and Modified DRASTIC (Engel et al., 1996) Classifications

DRASTIC (Aller et al., 1987)	DRASTIC (Engel et al., 1996) Low (km²)	DRASTIC (Engel et al., 1996) Moderate (km²)	DRASTIC (Engel et al., 1996) High (km²)
Low (km²)	3.76	20.46	0.00
Moderate (km²)	–	13.99	24.45
High (km²)	–	0.00	7.80

Comparing intrinsic DRASTIC outputs against specific SI vulnerability outputs identified spatial differences (**Figures 10 and 11**). Applying Equation 7 yielded coincidence rates (T_c) of 41.70% for the DRASTICLU model and 33.30% for the SI model against observed nitrate data (**Tables 10 and 11**).

Table 10
Cross-Tabulation Matrix Between Nitrate Concentrations and Calibrated DRASTIC (DRASTICLU) Index

DRASTICLU Index	Nitrates: 0–25 mg/L	Nitrates: 25–50 mg/L	Nitrates: 50–500 mg/L
Low	2	3	1
Moderate	10	9	5
High	–	1	4

Map Removal Sensitivity Analysis (MRSA)

Map removal sensitivity analysis demonstrated that vulnerability indices are disproportionately influenced by net recharge (R) and topography (T). Specifically, net recharge in the DRASTICLU model exhibited a low variation index (1.71%), while topography in the SI model

https://doi.org/10.4314/orapj.v7i10.91

showed a variation index of 2.98%. These parameters mask the direct impact of land use (LU), which yielded minimal variation indices of 0.82% and 0.96%, respectively **(Tables 12 and 13)**.

Figure 10:
Areas of agreement and disagreement between the SI and DRASTIC (Aller et al. 1996) models

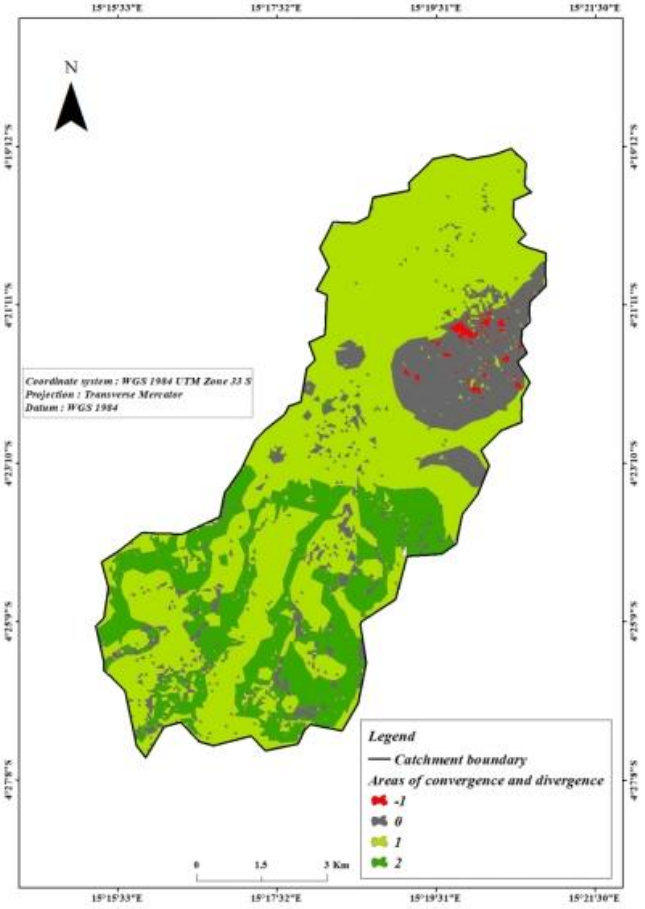


Table 11
Cross-Tabulation Matrix Between Nitrate Concentrations and Susceptibility Index (SI)

SI Index	Nitrates: 0–25 mg/L	Nitrates: 25–50 mg/L	Nitrates: 50–500 mg/L
Low	–	7	6
Moderate	–	6	7
High	–	4	6

Table 12
One-Map Removal Sensitivity Analysis Statistics for the DRASTICLU Model

Parameter Removed	Min Variation (%)	Max Variation (%)	Mean Variation (%)	Standard Deviation (SD)
D	0.00	4.42	0.99	0.62
R	0.96	3.58	1.71	0.51
A	0.00	1.14	0.15	0.16
S	0.00	0.96	0.50	0.36
T	0.59	1.70	1.22	0.24
I	0.00	1.53	0.38	0.20
C	1.05	1.55	1.39	0.08
LU	0.00	2.64	0.82	0.53

Figure 11:
Areas of agreement and disagreement between the SI and DRASTIC (Engel et al. 1996) models

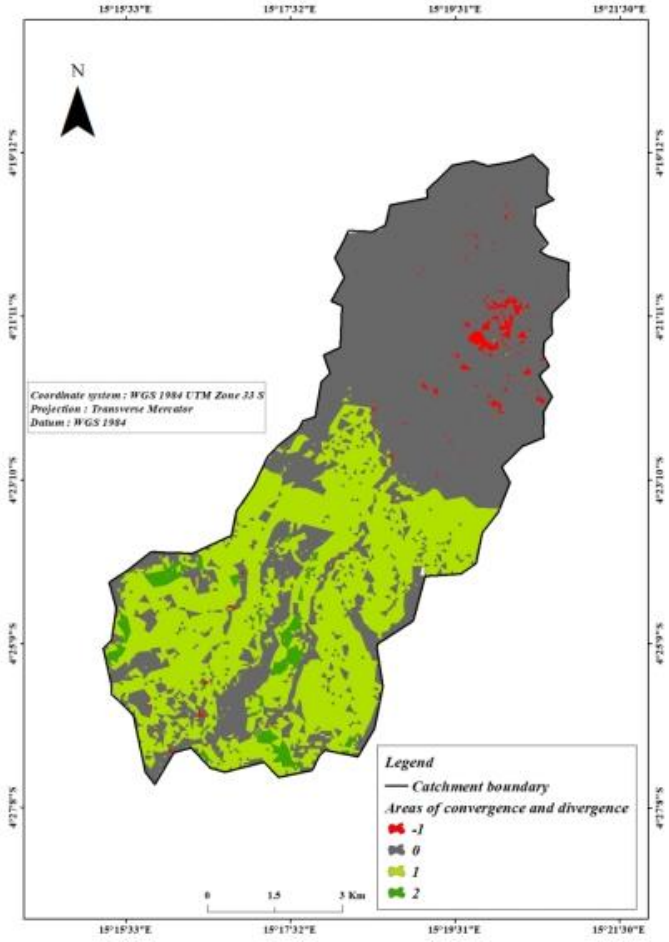


Table 13
One-Map Removal Sensitivity Analysis Statistics for the SI Model

Parameter Removed	Min Variation (%)	Max Variation (%)	Mean Variation (%)	Standard Deviation (SD)
D	0.00	14.63	1.64	1.43
R	0.45	7.06	1.94	0.65
A	0.00	6.11	1.70	0.87
T	0.03	4.60	2.98	1.35
LU	0.00	5.00	0.96	0.88

Single-Parameter Sensitivity Analysis (SPSA)

Single-parameter sensitivity analysis confirmed that theoretical parameter weights diverge substantially from effective weights calculated under local field conditions. The effective weight for net recharge (R) was significantly overestimated relative to its theoretical weight in both the DRASTICLU model (22.66% versus 14.28%; **Table 14**) and the SI model (21.20% versus 27.78%; **Table 15**). Conversely, hydraulic conductivity (C), representing horizontal subsurface flow, received an effective weight of only 2.75%, far below its theoretical weight of 10.71%.

https://doi.org/10.4314/orapj.v7i10.91

Table 14
Single-Parameter Sensitivity Analysis (SPSA) Statistics for the DRASTICLU Model

Parameter	Theoretical Weight	Theoretical Weight (%)	Effective Weight (Mean %)	Effective Weight (Min %)	Effective Weight (Max %)	Standard Deviation (SD)
D	5	17.85	16.91	3.06	34.24	6.16
R	4	14.28	22.66	17.30	35.64	3.78
A	3	10.71	13.25	9.78	20.51	1.41
S	2	7.14	9.71	5.76	17.82	3.33
T	1	3.57	3.94	0.54	8.77	1.72
I	5	17.85	13.31	7.77	23.25	2.94
C	3	10.71	2.75	1.63	5.08	0.62
LU	5	17.85	17.50	2.40	34.78	4.93

Table 15
Single-Parameter Sensitivity Analysis (SPSA) Statistics for the SI Model

Parameter	Theoretical Weight	Theoretical Weight (%)	Effective Weight (Mean %)	Effective Weight (Min %)	Effective Weight (Max %)	Standard Deviation (SD)
D	0.186	18.60	14.98	2.85	32.71	5.94
R	0.212	21.20	27.78	21.80	48.24	2.62
A	0.258	25.80	26.80	17.75	44.47	3.54
T	0.121	12.10	8.10	1.52	27.25	5.47
OS	0.222	22.20	22.38	0.00	38.08	4.74

DISCUSSION

Explanation of Results

Assessing aquifer vulnerability requires high-resolution, locally calibrated hydrogeological data to produce actionable maps for urban planning. Obtaining deep subsurface data in Kinshasa presented significant logistical challenges, and existing geological logs did not fully capture small-scale lithological heterogeneity. Consequently, spatial interpolation methods introduced minor predictive uncertainties. Nevertheless, integrating multi-parameter datasets established a robust methodological framework.

Initial physicochemical parameters (electrical conductivity, total dissolved solids, and pH) indicated high mineralization and acidic groundwater conditions (pH < 4). As noted by Backalowicz (1979, cited in Ndembo, 2009), groundwaters hosted in pure siliceous sands and sandstone formations are characteristically acidic due to the dissolution of carbonic acid derived from atmospheric CO_2 and humic/fulvic acids released during organic matter decomposition in humid tropical soils.

The standard DRASTIC model delineated three intrinsic vulnerability tiers. Applying Engel et al.'s (1996) modified classification revealed that the standard model underestimates sensitivity across lowland areas. Both models identify the low-lying plains and river valleys as the most sensitive hydrogeological zones. These areas feature shallow water tables, highly permeable Quaternary sandy alluvium, and gentle topographic slopes (< 2%), spanning the densely populated townships of Limete, Kalamu, Ngaba, Makala, Lemba, Ngiri-Ngiri, Bumbu, and Selembao.

The Susceptibility Index model, which incorporates land-use parameters, demonstrated that 83.50% of the aquifer system is vulnerable to surface contamination. Intensive agricultural activities, unmanaged domestic wastewater, unsealed pit latrines (Massawe et al., 2017), and municipal solid waste used to stabilize mega-gullies in Mont-Ngafula and Selembao (Makanzu Imwangana et al., 2022, 2025) act as primary pollution sources. Soluble pollutants infiltrate rapidly during high-intensity tropical rainfall events (Matungila, 2023; Mfumu et al., 2016).

Validation against borehole nitrate data revealed that the DRASTICLU model achieved a higher coincidence rate (41.70%) than the SI model (33.30%), indicating that DRASTICLU more accurately reflects diffuse urban nitrate loading. Sensitivity analyses, however, highlighted structural limitations in standard parametric weights derived in the United States, which overemphasize net recharge while underrepresenting lateral groundwater flow and specific land-use pressures. Adapting index weights to local tropical hydrogeological conditions is therefore essential for future assessments. Furthermore, uneven spatial distribution of monitoring boreholes—

largely absent in areas serviced by REGIDESO—partially accounts for lower statistical coincidence rates.

Comparison with Previous Studies

Few regional studies have applied integrated parametric vulnerability models in the DRC (Mbuluyo et al., 2017; Mfumu et al., 2016). Broader international comparisons confirm that standard DRASTIC models require localized calibration and sensitivity testing (Aminreza et al., 2014; Ghazavi & Ebrahimi, 2015; Hu et al., 2018; Ifediegwu & Chibuike, 2021; Rahman, 2008).

Our findings align with Chenini et al. (2015), who demonstrated that Engel et al.'s (1996) modified classification increases sensitivity identification in vulnerable alluvial settings. While previous researchers (Jesiya & Gopinath, 2019; Mfumu et al., 2016) modified DRASTIC by reweighting parameters or omitting poorly correlated layers (e.g., aquifer media and vadose zone impact), our study retained all core parameters in accordance with Hamza et al. (2015) to preserve comprehensive baseline evaluation.

CONCLUSION

This study assessed the intrinsic and specific vulnerability of the aquifer system in the Funa catchment using GIS-based DRASTIC, DRASTICLU, and SI parametric models. Spatial integration of hydrogeological, climatic, topographic, and land-use data successfully delineated natural groundwater protection zones across the basin.

The standard DRASTIC model indicated that moderate vulnerability dominates the catchment, whereas Engel et al.'s (1996) modified classification significantly expanded high-vulnerability zones. The SI and DRASTICLU models confirmed that low-lying alluvial plains are highly vulnerable to surface-derived anthropogenic pollution due to shallow water tables, permeable sandy soils, and intense urbanization lacking adequate sanitation infrastructure. Sensitivity analyses revealed that standard parameter weights overemphasize net recharge, underscoring the necessity of localized weight optimization.

To safeguard public health and groundwater quality, municipal authorities must establish strict groundwater governance frameworks, register private boreholes, enforce sanitary protection zones, and implement sustainable solid waste and wastewater management systems. These findings provide critical decision-support tools for urban land-use planning and environmental management in Kinshasa.

Use of Artificial Intelligence (AI) Declaration: The authors declare that no artificial intelligence tools, software, or language models were utilized at any stage in the preparation, execution, or reporting of this research.

Acknowledgments: The authors express their gratitude to colleagues within the Geomatics laboratory for their invaluable assistance with spatial data processing and map preparation.

Authors' Contributions

i. Iyeli, L.P.: Conceptualization, Investigation, Methodology, Data curation, Software, Visualization.
ii. Ndongela, M.J.: Software, Visualization.
iii. Tangou, T.T.: Writing – review & editing.
iv. Gizanga, V.R.: Writing – review & editing.
v. Makanzu, I.F.: Supervision, Writing – review & editing.
vi. Mfumu, K.A.: Supervision, Writing – review & editing.

Data Availability Statement: The data supporting the findings of this study are available from the corresponding author upon reasonable request.

Ethical Approval: Ethical approval was not required for this study as it did not involve human participants, personal data, or animal testing. However, formal research clearance was granted by the Faculty of Science and Technology at the University of Kinshasa (UNIKIN) to conduct the field activities.

Funding: This research was entirely self-funded by the authors. No external financial assistance or logistical support was received.

Conflicts of Interest: The authors declare that they have no conflicts of interest.

ORCID iDs:

Iyeli, L. P.[1,2]: https://orcid.org/0009-0003-3533-8167
Ndongela, M. J.[4]: https://orcid.org/0009-0005-4566-4569
Mfumu, K. A.[3]: https://orcid.org/0000-0003-0702-1261
Tangou, T. T.[1,2,3]: https://orcid.org/0009-0003-6788-9684
Gizanga, V. R.[2]: https://orcid.org/0009-0009-0692-8348
Makanzu, I. F.[4,5]: https://orcid.org/0000-0002-0793-7969

Open Access: This original article is distributed under the Creative Commons Attribution Non-Commercial (CC BY-NC 4.0) license. This license permits people to distribute, remix, adapt, and build upon this work non-commercially and license their derivative works on different terms, provided the original work is properly cited, appropriate credit is given, any changes made are indicated, and the use is non-commercial. See: https://creativecommons.org/licenses/by-nc/4.0/.

REFERENCES

Aller, L., Lehr, J. H., Petty, R., & Bennett, T. (1987). *DRASTIC: A standardized system to evaluate ground water pollution potential using hydrogeological settings* (EPA/600/2-87/035). U.S. Environmental Protection Agency.

Alsharifa, H. (2017). Assessing the groundwater vulnerability in the upper aquifers of Zarqa River Basin, Jordan using DRASTIC, SINTACS and GOD methods. *International Journal of Water Resources and Environmental Engineering*, 9(2), 44–52. https://doi.org/10.5897/IJWREE2016.0691

Amharref, M., Aassine, S., Bernoussi, A. S., & Haddouchi, B. Y. (2007). Cartographie de la vulnérabilité à la pollution des eaux souterraines: Application à la plaine du Gharb (Maroc). *Revue des Sciences de l'Eau / Journal of Water Science*, 20(2), 185–199. https://doi.org/10.7202/015812ar

Aminreza, N., Biswajeet, P., & Moshen, D. (2014). Groundwater vulnerability assessment using an improved DRASTIC method in GIS. *Resources, Conservation and Recycling*, 86, 95–104. https://doi.org/10.1016/j.resconrec.2014.02.008

Amrani, S., Hinaje, S., & Gharmane, Y. (2019). Application of the parametric methods (DRASTIC and SI) for the study of the vulnerability in the potential pollution by nitrates of the superficial groundwater of Timahdite-Almis Guigou (Middle Atlas, Morocco). *Revue des Sciences de l'Eau*, 32(4), 311–326. https://doi.org/10.7202/1067307ar

Chenini, I., Zghibi, A., & Kouzana, L. (2015). Hydrogeological investigations and groundwater vulnerability assessment and mapping for groundwater resource protection and management: State of the art and a case study. *Journal of African Earth Sciences*, 109, 22–36. https://doi.org/10.1016/j.jafrearsci.2015.05.008

Courbe, L. (2023). *Etude du développement des ravins urbains à Kinshasa à l'aide d'images satellites* [Master's thesis, Liège Université Sciences].

Davies, T. C. (2015). Urban geology of African megacities. *Journal of African Earth Sciences*, 110, 188–226. https://doi.org/10.1016/j.jafrearsci.2015.06.012

Dekkiche, I., & Mezaour, A. (2019). Etude comparative de trois méthodes pour la cartographie de la vulnérabilité de l'aquifère alluviale à la pollution, plaine alluviale de Khemis Miliana. *University of Science and Technology Houari Boumediene*, 102 p.

Egoroff, A. (1947). *Bulletins du service géologique de Léopoldville de la Direction Générale des Affaires Economiques*. Service Géologique du Congo Belge.

Egoroff, A. (1995). *Carte géologique de Léopoldville*. Service Géologique du Congo Belge et du Rwanda-Urundi, 1–15.

Engel, B. A., Navulur, K. C. S., Cooper, B. S., & Hahn, L. (1996). Estimating groundwater vulnerability to non-point source pollution from nitrates and pesticides on a regional scale. In *Subsurface Water Contamination* (IAHS Publication No. 235, pp. 521–526). IAHS Press.

Ewodo, M. G., Ombolo, A., Bon, A. F., Ntep, F., & Bineli, E. (2016). Apport des méthodes paramétriques DRASTIC, GOD et SI à l'évaluation de la vulnérabilité intrinsèque dans les aquifères du bassin versant de l'Abiergué (région de Yaoundé). *REVUE CAMES*, 4(2), 2424–7235.

Falasi, N. J. (2018). *Pollution de la rivière N'djili et contraintes de gestion des sols autours du pool Malebo (cas du site agricole Masina rail 1/Kinshasa)* [Master's thesis, University of Liège].

Frind, E. O., Molson, J. W., & Rudolph, D. L. (2006). Well vulnerability: A quantitative approach for source water protection. *Ground Water*, 44(5), 732–742. https://doi.org/10.1111/j.1745-6584.2006.00230.x

Ghazavi, R., & Ebrahimi, Z. (2015). Assessing groundwater vulnerability to contamination in an arid environment using DRASTIC and GOD models. *Environmental Earth Sciences*, 74(12), 7741–7753. https://doi.org/10.1007/s13762-015-0813-2

Gizanga, V. R., Musibono, E. A. D., Aleke, A. L., & Milau, E. F. (2016). Contribution à l'évaluation de la qualité des effluents industriels et de leurs impacts sur les milieux récepteurs (ville de Kinshasa - République Démocratique du Congo, RDC). *International Journal of Innovation and Scientific Research*, 21(2), 360–366.

Gogu, R. C., & Dassargues, A. (2000). Current trends and future challenges in groundwater vulnerability assessment using overlay and index methods. *Environmental Geology*, 39(6), 549–559. https://doi.org/10.1007/s002540050466

Guetter, P., & Kutzbach, J. (1990). A modified Köppen classification applied to model simulations. *Climate Change*, 16(2), 193–216. https://doi.org/10.1007/BF00145828

Hamza, S. M., Ahsan, A., Imteaz, M. A., Rahman, A., Mohammad, T. A., & Ghazali, A. H. (2015). Accomplishment and subjectivity of GIS-based DRASTIC groundwater vulnerability assessment method: A review. *Environmental Earth Sciences*, 73(7), 3063–3076. https://doi.org/10.1007/s12665-014-3610-x

Hansa, R., Rohit, G., & Urmila, B. (2020). Modification and optimization of DRASTIC model for groundwater vulnerability and contamination risk assessment for Bhiwadi region of Rajasthan, India. *Environmental Earth Sciences*, 79(6), 136. https://doi.org/10.1007/s12665-020-8874-z

Ifediegwu, S. I., & Chibuike, I. E. (2021). GIS-based evaluation of shallow aquifer vulnerability to pollution using DRASTIC model: A case study on Abakaliki, southeastern Nigeria. *Arabian Journal of Geosciences*, 14(20), 2097. https://doi.org/10.1007/s12517-021-08811-8

Ilunga, J. M., Devarajan, N., Le Faucheur, S., Mputu, J. K., Atibu, E. K., Sivalingam, P., Prabakar, K., Mpiana, P. T., Wildi, W., & Poté, J. (2013). Effects of untreated hospital effluents on the accumulation of toxic metals in sediments of receiving system under tropical conditions: Case of south India and Democratic Republic of Congo. *Chemosphere*, 93(6), 1070–1076. https://doi.org/10.1016/j.chemosphere.2013.05.074

Jesiya, M., & Gopinath, G. (2019). Groundwater vulnerability assessment of a humid tropical river basin using DRASTIC model and GIS. *Groundwater for Sustainable Development*, 9, 100217. https://doi.org/10.1016/j.gsd.2019.100217

Kaleka, N. E. (2021). *La gestion des eaux, condition d'équilibre de l'habitat collinaire. Kindele (Kinshasa)* [Doctoral dissertation, Université de Liège & Université Libre de Bruxelles].

Kasuku, W., Bouland, C., De Brouwer, C., Mareschal, B., Mulaji, C., Malumba, M., Monama, O., Epumba, B., & Kitambala, A. (2016). Etude de l'impact sanitaire et environnemental des déchets hospitaliers dans 4 établissements hospitaliers de Kinshasa en RDC. *Déchets, Sciences et Techniques*, 71, 25–33. https://doi.org/10.4267/dechets-sciences-techniques.3385

Khemiri, S., Khnissi, A., Alaya, M. B., Saidi, S., & Zargouni, F. (2013). Using GIS for the comparison of intrinsic parametric methods assessment of groundwater vulnerability to pollution in scenarios of semi-arid climate: The case of Foussana groundwater in the central of Tunisia. *Journal of Water Resource and Protection*, 5(9), 835–845. https://doi.org/10.4236/jwarp.2013.59085

Lemba, S. D. (2013). *Assessment of land use dynamics of the N'djili catchment in DR Congo: Implication for catchment planning* [Master's thesis, University of Zimbabwe].

Liggett, J. E., & Talwar, S. (2009). Groundwater vulnerability assessments and integrated water resource management. *Streamline Watershed Management Bulletin*, 13(1), 18–29.

Lodwick, W. A., Monson, D., & Svoboda, L. (1990). Attribute error and sensitivity analysis of map operations in geographical information systems: Suitable methods. *International Journal of Geographical Information Systems*, 4(4), 413–428. https://doi.org/10.1080/02693799008941557

Makanzu Imwangana, F. (2023). *Origine et contrôle de l'érosion ravinante à Kinshasa (RD Congo)*. Éditions L'Harmattan.

Makanzu Imwangana, F., Kamosi Zola, B., Mbiya Kangudia, J., & Pangu Sanghy, S. (2025). Gully erosion associated with peri-urbanisation: Focus on the catchments around Kimwenza in the south of Kinshasa (DR Congo). *East African Journal of Environment and Natural Resources*, 8(2), 136–166. https://doi.org/10.37284/eajenr.8.2.3160

Makanzu Imwangana, F., Kiangebeni, C., Ilito, P. D., & Matungila Juve, J. (2022). Preuve et impact d'un auto-aménagement urbain dans le bassin versant de la Lukunga à Kinshasa. *Revue Africaine d'Environnement et d'Agriculture*, 5(4), 85–96.

Makanzu Imwangana, F., Vandecasteele, I., Ozer, P., Trefois, P., & Moeyersons, J. (2015). The origin and control of mega-gullies in Kinshasa (DR Congo). *Catena*, 125, 38–49. https://doi.org/10.1016/j.catena.2014.09.019

Massawe, S. L., Komakech, H. C., Lawrence, M., & Ijumba, J. N. (2017). Impact of human activities on groundwater vulnerability in Hombolo catchment, Dodoma, Tanzania. *Physics and Chemistry of the Earth, Parts A/B/C*, 100, 363–372. https://doi.org/10.1016/j.pce.2017.03.003

Matumona Seya, C., Lokanda Mpiangeli, P., Kamosi Zola, B., Kilensele Muwele, T., & Makanzu Imwangana, F. (2025). Impact de l'érosion ravinante sur la fertilité des sols des zones maraîchères des quartiers Kimwenza et Matadi Mayo dans la Commune de Mont-Ngafula à Kinshasa. *Revue Africaine d'Environnement et d'Agriculture*, 8(4), 134–149. https://doi.org/10.4314/rafea.v8i4.12

Matungila, J. (2023). *Evaluation et Cartographie de la vulnérabilité des eaux souterraines du bassin versant de la Lukunga à Kinshasa* [Master's thesis, University of Kinshasa].

Matungila, J., Hallal Dahbia, D., Makanzu Imwangana, F., & N'zau Umba-di-Mbudi, C. (2026). Cartographie de la vulnérabilité des eaux souterraines du bassin versant de Lukunga dans la ville de Kinshasa. *Revue Congolaise des Sciences et Technologies*, 5(1), 58–69. https://doi.org/10.59228/rcst.026.v5.i1.221

Matungila, J., Hallal Dahbia, D., Ouahiba, A., Tshimanga, R., Makanzu Imwangana, F., & N'zau Umba-di-Mbudi, C. (2025). Groundwater vulnerability mapping and health risk assessment of essential

elements deficiencies in groundwater in the Lukunga watershed of Kinshasa city. *Geomatics, Landmanagement and Landscape*, 4, 167–186. https://doi.org/10.15576/GLL/212639

Mbuluyo, M., Mushauri, F., & M'putu, P. (2017). Cartographie de la vulnérabilité à la pollution de la nappe souterraine d'Isiro (Nord-est de la RD Congo) à partir de la méthode DRASTIC. *Afrique Science*, 13(3), 125–139.

Meyzonnat, G. (2012). *Estimation de la vulnérabilité de l'aquifère au roc de la zone Bécancour (Centre-du-Québec)* [Master's thesis, Université du Québec à Montréal].

Mfumu, K. A. (2016). *Assessing nitrate pollution in the Kinshasa groundwater system using a hybrid approach* [Doctoral dissertation, Université Catholique de Louvain].

Mfumu, K. A., Vanclooster, M., & Ndembo, L. J. (2016). Assessing groundwater vulnerability in the Kinshasa region, DR Congo, using a calibrated DRASTIC model. *Journal of African Earth Sciences*, 126, 13–22. https://doi.org/10.1016/j.jafrearsci.2016.11.025

Mindele, L. U. (2016). *Caractérisation et tests de traitement des déchets ménagers et boues de vidange par voie anaérobie et compostage pour la ville de Kinshasa* [Doctoral dissertation, University of Liège].

Miti, T. F., & Mukanu, A. (2021). Analyse de la morphographie du bassin versant de la Funa à l'aide du SIG et de la Télédétection. *HAL Open Science*, hal-04627602.

Napolitano, P., & Fabbri, A. (1996). Single-parameter sensitivity analysis for aquifer vulnerability assessment using DRASTIC and SINTACS. *HydroGIS 96: Application of Geographic Information Systems in Hydrology and Water Resources Management*, 559–566.

Ndembo, L. J. (2009). *Apport des outils hydrogéochimiques et isotopiques à la gestion de l'aquifère du Mont-Amba (Kinshasa, République Démocratique du Congo)* [Doctoral dissertation, Université d'Avignon et des Pays de Vaucluse & Université de Kinshasa].

Ndolo, P. G. (2015). *GIS-Based soil erosion modeling and sediment yield of the N'Djili River Basin, Democratic Republic of Congo* [Master's thesis, Colorado State University].

Neukum, C., & Azzam, R. (2009). Impact of different methodology on groundwater vulnerability maps. *Environmental Earth Sciences*, 58(3), 669–681. https://doi.org/10.1007/s12665-008-0067-1

Ojeda-Olivares, E. A., Belmonte Jiménez, S. I., Sandoval Torres, S., Campos Enríquez, J. O., Tiefenbacher, P., & Takaro, T. K. (2020). A simple method to evaluate groundwater vulnerability in urbanizing agricultural regions. *Journal of Environmental Management*, 270, 110164. https://doi.org/10.1016/j.jenvman.2020.110164

Peel, M. C., Finlayson, B. L., & McMahon, T. A. (2007). Updated world map of the Köppen-Geiger climate classification. *Hydrology and Earth System Sciences*, 11(5), 1633–1644. https://doi.org/10.5194/hess-11-1633-2007

Rahman, A. (2008). A GIS based DRASTIC model for assessing groundwater vulnerability in shallow aquifer in Aligarh, India. *Applied Geography*, 28(1), 32–53. https://doi.org/10.1016/j.apgeog.2007.07.008

Ribeiro, L. (2000). *Index de susceptibilidade à poluição dos aquíferos* [Doctoral dissertation, Universidade Nova de Lisboa].

Rizka, M. (2018). Comparative studies of groundwater vulnerability assessment. *IOP Conference Series: Earth and Environmental Science*, 118(1), 012018. https://doi.org/10.1088/1755-1315/118/1/012018

Saaty, T. L. (2008). Decision making with the analytic hierarchy process. *International Journal of Services Sciences*, 1(1), 83–98. https://doi.org/10.1504/IJSSCI.2008.017590

Seguin, J. J., Baydry, D., & Platel, J. P. (2002). *Cartographie de la vulnérabilité des systèmes aquifères de l'Aquitaine* (BRGM Report No. 02EAU207). Bureau de Recherches Géologiques et Minières.

Simboro, A. (2016). *Gestion quantitative et qualitative des ressources en eau dans la plaine alluviale de Karfiguéla à l'aide d'un SIG: Etude de la recharge induit de la nappe et sa vulnérabilité à la pollution* [Master's thesis, 2IE Burkina Faso].

Simeneh, S. M., & Megersa, O. D. (2021). Assessment of groundwater vulnerability mapping methods for sustainable water resource management: An overview. *Journal of Water and Land Development*, 51, 195–204. https://doi.org/10.24425/jwld.2021.139029

UNESCO World Water Assessment Programme. (2016). *The United Nations World Water Report 2016: Water and Jobs*. United Nations Educational, Scientific and Cultural Organization.

Xiaojing, H., Chuanming, M., Huihui, Q., & Xu, G. (2018). Groundwater vulnerability assessment using the GALDIT model and the improved DRASTIC model: A case in Weibei Plain, China. *Environmental Science and Pollution Research*,

25(34), 34120–. https://doi.org/10.1007/s11356-018-3196-3